A Coordination Strategy to Realize a Sextuply Bonded Complex

Yue Chen,[a,b] Jun-ya Hasegawa,[a,b]* Kazuya Yamaguchi,[c] Shigeyoshi Sakaki[d]*

Synthesis of higher-order multiple bond is a great challenge in chemistry. However, no stable compound with a sextuple bond has been reported, except for Mo_2 in an inert matrix at low temperature. Here, we propose a strategy to construct a sextuple bond in a dinuclear transition metal complex based on the complete active space second-order perturbation theory (CASPT2) and density functional theory calculations. When the dinuclear core M_2 (M = W, Mo, and Re^+) is capped by two neutral electron-donating ligands at both M-M ends, a sextuple bond can be realized. The proposed ligands stabilize the M_2 core by the coordination, conserve the six bonding orbitals in the occupied space, and suppress the weight of the δ-δ* excited electron configuration. Calculated large formation energies of these complexes indicate the large possibility of the synthesis. Electronic structure and sextuply bonding interactions are analyzed in detail.

1. Introduction

To create the highest multiple bond in a stable compound has been a great interest to chemists for decades. In main group elements, the triple bond was supposed to be the limit of multiple bond for nearly 50 years.[1] Recently, the quadruple bond was suggested to exist in C_2 and its isoelectronic molecules (CN^+, BN, and CB^-).[2-4] In transition metal element, the quadruple bond was found in $[Re_2Cl_8]^{2-}$ by Cotton et al. in 1964.[5] Four decades later, the range of bond multiplicity was extended to five by the synthesis of a dichromium complex in 2005.[6] After that, many stable quadruply and quintuply bonded dinuclear transition metal complexes have been synthesized.[7-23]

Though quadruple bonds do not exhibit reactivity, it is interesting that some of quintuple bonds are highly reactive,[24-34] suggesting that the sextuple bond exhibits new feature. However, the synthesis of the sextuple bond is still a great challenge in chemistry. Only limited knowledge of the sextuple bond is available both in experiment and theory. A sextuple bond could be formed with five n*d* orbitals and one (n+1)*s* orbital of a transition metal in a diatomic molecule such as Cr_2, Mo_2, and W_2.[35-46] Thus, twelve atomic orbitals form six bonding molecular orbitals (MOs) ($\sigma_{(n+1)s}$, σ_{nd}, two π_{nd}, and two δ_{nd}) and six anti-bonding MOs ($\sigma^*_{(n+1)s}$, σ^*_{nd}, two π^*_{nd}, and two δ^*_{nd}); see Fig. 1. If the six bonding MOs are doubly occupied and their anti-bonding counterparts are unoccupied, a sextuple bond is formed. In other words, the closed-shell singlet electron configuration $\sigma^2_{(n+1)s}\sigma^2_{nd}\pi^4_{nd}\delta^4_{nd}\sigma^{*0}_{(n+1)s}\sigma^{*0}_{nd}\pi^{*0}_{nd}\delta^{*0}_{nd}$ provides the sextuple bond in a formal sense; hereafter, we use "S_0 state" for an electronic state bearing this closed-shell electron configuration as a dominant term. The present study focuses on transition metals, but not on actinides that are also expected to be useful in forming a metal-metal multiple bond with 5*f* orbitals.[47-52]

Roos et al. proposed a concept of effective bond order (EBO) to evaluate the bond order as follows.[53, 54] For a single bond, EBO is defined as

$$\mathrm{EBO} = (\eta_b - \eta_a)/2 \quad (1)$$

where η_b and η_a are occupation numbers of bonding and anti-bonding MOs, respectively. The occupation number is usually calculated by multi-configurational wave function method for strongly correlated systems. For a multiply bond, the total EBO is the summation of the contributions from each bond. In a transition metal sextuple bond, the EBOs of σ_{nd}, π_{nd}, δ_{nd}, and $\sigma_{(n+1)s}$ contribute to the total EBO. The EBO is non-integer in many cases. A multiplicity of a bond is defined as the lowest integer value larger than the EBO. For example, the EBO of the Re-Re quadruple bond in $[Re_2Cl_8]^{2-}$ was calculated to be 3.2 by a multi-configurational method.[53, 54]

After systematic theoretical studies, Roos et al. concluded that only Mo_2 and W_2, whose EBOs are both 5.2, have a sextuple bond in diatomic molecules.[54] In the Cr_2 case, the calculated EBO value (3.5) suggested that this molecule has a quadruple bond. This is true because the strong $\delta - \delta^*$ electron correlation reduces the bond order.[55] In experiment, only Mo_2 was synthesized, but in an inert

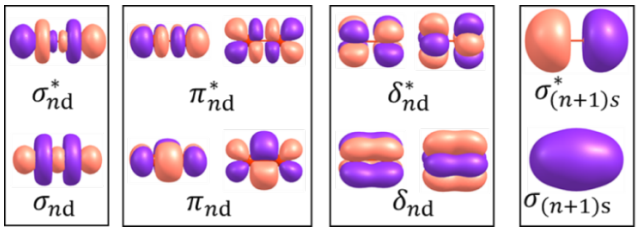

Fig. 1 Molecular orbitals contributing to sextuple bond in transition metal element.

[a] *Institute for Catalysis, Hokkaido University, Kita 21 Nishi 10, Kita-ku, Sapporo 001-0021, Japan, E-mail: hasegawa@cat.hokudai.ac.jp*
[b] *CREST, Japan Science and Technology Agency, 4-1-8, Honcho, Kawaguchi-shi, Saitama 332-0012, Japan.*
[c] *Department of Applied Chemistry, School of Engineering, The University of Tokyo,7-3-1 Hongo, Bunkyoku, Tokyo, Japan*
[d] *Fukui Institute for Fundamental Chemistry, Kyoto University, 34-4, Takano-Nishihiraki, Sakyo-ku, Kyoto 606-8103, Japan, E-mail: sakaki.shigeyoshi.47e@st.kyoto-u.ac.jp*
Electronic Supplementary Information (ESI) available: Computational details; Sextuply bonded state of Re_2^{2+}; Twisted geometry of $O_4(M_2)O_4$; Charge transfer from O_4 ligands to M_2; Electronic stats of the side-on-like complexes; Cartesian Coordinate.

matrix at low temperature.[41] As far as we know, neither experimental nor theoretical studies have reported a stable sextuply bonded compound.

In this work, we propose a strategy to realize a sextuple bond in stable dinuclear transition metal complexes. In our strategy, the M_2 core (M = W, Mo, Re^+ , and Tc^+) is capped by two neutral electron-donating tetradentate ligands at both M-M ends. The complete active space self-consistent field (CASSCF) with second-order perturbation theory (CASPT2) calculations and the EBO analysis clearly show that a sextuple bond can be realized in dinuclear W, Mo, and Re^+ complexes. Both CASPT2/CASSCF and density-functional theory (DFT) results show that these complexes have large formation energies, indicating the large possibility of the synthesis.

2. Results and discussion

2.1. Sextuple bond in diatomic molecules

First, we show the bare metal dimer cases as the starting point. It is believed that among many transition metals, Cr, Mo, W, Mn^+, Tc^+, and Re^+ meet the requirements to form a sextuple bond.[1, 54] Previous theoretical studies demonstrated that the ground state of W_2 and Mo_2 are the S_0 state with a sextuple bond.[38-41, 43-46] Our DFT and CASPT2 calculations confirmed this conclusion. As shown in Table 1, the EBOs calculated with CASSCF for W_2 and Mo_2 in the S_0 state were 5.15 and 5.11, respectively. To our knowledge, Re_2^{2+} and Tc_2^{2+} have not been studied. At the DFT level, Re_2^{2+} has a meta-stable S_0 ground state with an equilibrium Re-Re distance of 2.005 Å, but its formation from two Re^+ cations is endothermic by 96.6 kcal/mol. The CASPT2 calculation also predicted instability, indicating that the synthesis of sextuply bonded Re_2^{2+} is difficult; see Fig. S1 in ESI. The instability of Re_2^{2+} in the S_0 state is attributed to the Coulomb repulsion between the two Re^+ cations. Our coordination strategy works for stabilizing the Re_2^{2+} structure, as will be described below.

In the case of Tc_2^{2+}, the lowest energy triplet state is more stable than the S_0 state by 13.2 and 14.5 kcal/mol at the DFT and CASPT2 levels, respectively. The δ_{nd}^* MOs have a lot of electron occupation because the energy level of the $\sigma_{(n+1)s}$ MO is higher than that of the δ_{nd}^* MO; see Fig. 2. As a result, the EBO of Tc_2^{2+} calculated by CASSCF is only 4.11; see Table 1. The formation of Tc_2^{2+} is endothermic by 115.2 and 125.3 kcal/mol at the DFT and CASPT2 levels, respectively. From these results, a sextuple bond is formed in diatomic W_2 and Mo_2 molecules, but not in diatomic Re_2^{2+} and Tc_2^{2+}.

2.2. Coordination strategies to realize a sextuple bond in a stable complex

Coordination of M_2 with electron-accepting ligand. To make a sextuple bond in a dinuclear complex by utilizing the coordination of ligands, the use of an electron-accepting ligand such as cyclopentadienyl (Cp)[56] and benzene(C_6H_6)[57] was theoretically proposed in pioneering works. The computational results certainly showed that $CpRe_2Cp$ in the singlet state has a sextuple bond. However, a triplet state with a quintuple bond was calculated to be the ground state.[56]

Table 1. Effective bond order[a] (EBO) of metal-metal bond.

M[b]	L[b]	$EBO_{\sigma_{nd}}$	$EBO_{\pi_{nd}}$	$EBO_{\delta_{nd}}$[c]	$EBO_{\sigma_{(n+1}}$	EBO
W	-	0.87	1.81	1.54 (0.77)	0.93	5.15
Mo	-	0.88	1.79	1.51 (0.75)	0.93	5.11
Re^+	-	0.87	1.75	1.20 (0.60)	0.88	4.70
Tc^+	-	0.86	1.73	1.04 (0.52)	0.48	4.11
W	O_4	0.87	1.82	1.52 (0.76)	0.95	5.17
Mo	O_4	0.87	1.79	1.47 (0.74)	0.97	5.10
Re^+	O_4	0.81	1.76	1.23 (0.62)	0.96	4.76
Tc^+	O_4	0.85	1.75	1.09 (0.55)	0.49	4.18
W	O_2N_2	0.86	1.83	1.55 (0.78)	0.97	5.22
Mo	O_2N_2	0.85	1.79	1.44 (0.72)	0.99	5.07
Re^+	O_2N_2	0.85	1.79	1.53 (0.76)	0.97	5.13
Tc^+	O_2N_2	0.86	1.74	1.22 (0.61)	0.50	4.32
W	N_4	0.88	1.86	1.80 (0.90)	0.98	5.51
Mo	N_4	0.86	1.81	1.63 (0.81)	0.99	5.29
Re^+	N_4	0.88	1.84	1.88 (0.96)	0.98	5.58
Tc^+	N_4	0.44	1.75	1.91 (0.95)	0.49	4.59

[a] $EBO_{\sigma_{nd}}$, $EBO_{\pi_{nd}}$, $EBO_{\delta_{nd}}$, and $EBO_{\sigma_{(n+1)s}}$ are EBO for the σ_{nd}, π_{nd}, δ_{nd}, and $\sigma_{(n+1)s}$ bonds, and EBO is for the total bond order. [b] "M" and "L" denote metal and ligand, respectively. For the structures of the ligands, see Scheme 1. [c] For $EBO_{\delta_{nd}}$, the value in parentheses is the average value of two δ_{nd} bonds.

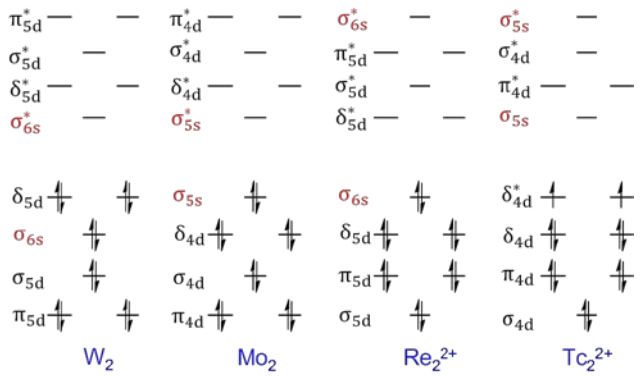

Fig. 2 Dominant electron configuration of M_2 (M=W, Mo, Re^+, and Tc^+).

The metal-metal bond in the ground state of $(C_6H_6)Cr_2(C_6H_6)$, $C_6H_6(Mo_2)C_6H_6$, and $C_6H_6(W_2)C_6H_6$ was calculated to be a quadruple bond rather than a sextuple bond.[57] The reason is that the metal-ligand interaction significantly changes the relative energies of bonding and anti-bonding MOs of the M-M moiety. As shown in Fig. 3A, the δ_{nd} and δ_{nd}^* orbitals are both stabilized significantly by the π* orbitals of benzene through back-donation interaction. In contrast, the $\sigma_{(n+1)s}$ and π_{nd} MOs are rather destabilized by the interactions with the π orbitals of benzene. As clearly seen in Fig 3B, only the δ_{nd} and δ_{nd}^* orbitals form bonding interactions with the benzene π* orbitals, while the $\sigma_{(n+1)s}$ and π_{nd} MOs have anti-bonding interactions with the benzene π orbitals. Because of spatial symmetry of MOs, the δ_{nd} and δ_{nd}^* MOs are only allowed to interact with the unoccupied MOs of benzene. As a result, the δ_{nd}^*

MO energy becomes lower than the $\sigma_{(n+1)s}$, and the electron population increases in the δ^*_{nd} MO rather than in the $\sigma_{(n+1)s}$ MO; see Fig. 3. See also Fig. S8 in ESI for orbital correlation diagram of the $C_6H_6(M_2)C_6H_6$ complex. To conserve the six metal-metal bonding MOs in the occupied space, an ideal condition is that the energy levels of the six bonding MOs shift uniformly by the ligand coordination. Considering the MOs of CpM_2Cp and $C_6H_6(M_2)C_6H_6$, the ligand used is requested not to stabilize the energy of the δ^*_{nd} MO more than that of $\sigma_{(n+1)s}$ MO. To satisfy this requirement, ligand should not have electron-accepting π*- and δ*- type MOs.

Sextuply bonded complexes with electron-donating ligand. On the basis of the previous studies and above consideration, we propose a strategy to achieve the sextuple bond in a dinuclear complex. The basic idea is to keep the $\sigma_{(n+1)s}$ MO being more stable in energy than the δ^*_{nd} MO by employing an electron-donating ligand (L) without electron-accepting MO; see Fig. 4A. In this work, we employed a neutral tetradentate ligand with an electron-donating property, such as 12-crown-4 ether (referred as L = O_4), considering four factors: (1) The tetradentate electron-donating ligand interacts uniformly with all these bonding and anti-bonding MOs, and the six bonding MOs are kept in the occupied space. (2) A neutral ligand must be used to suppress the formation of too strong metal-ligand interaction. Because the $\sigma_{(n+1)s}$ orbital is more diffuse than the n*d* orbitals, a strong coordination would destabilize the $\sigma_{(n+1)s}$ MO much more than the δ^*_{nd} MOs. (3) The charge transfer (CT) from ligand to metal can stabilize the total system, particularly in the Re_2^{2+} case. And, (4) The crown and aza-crown ether ligands, which are neutral tetradendate ligand, are easily available and widely used in the transition metal complex;[58, 59] see Scheme 1 for the structures.

As shown in Fig. 5A, the M_2 (M = W, Mo, Re^+, or Tc^+) moiety with two O_4 ligands affords an $O_4(M_2)O_4$ complex. Calculated potential energy change by the ligand coordination shows that the ligand binding stabilizes the total energy as shown in Fig. 5B. In all of the W_2, Mo_2, and Re_2^{2+} complexes, the ground-state has singlet spin multiplicity as shown in Table S2A in ESI. The S_0 configuration, which is illustrated in Fig. 4B, is kept being a dominant configuration in CASSCF wave function. For example, the weight of the S_0 configuration in the $O_4(Mo_2)O_4$ and $O_4(W_2)O_4$ complexes are 66.5% and 64.5%, respectively; see Table S2B in ESI for the other complexes.

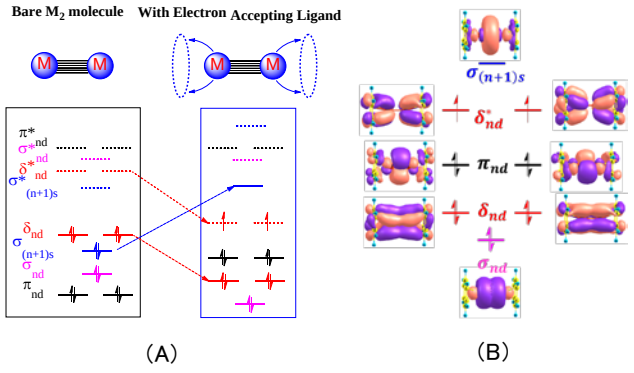

Fig. 3 (A) Orbital interaction between W_2 and two benzene ligands. (B) the MOs of $C_6H_6(W_2)C_6H_6$ with D_{6h} symmetry.

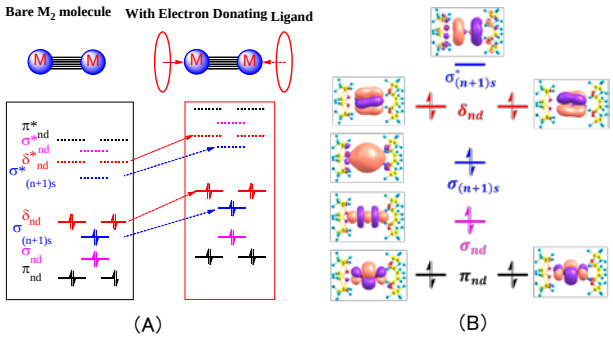

Fig. 4 (A) Orbital interactions between electron-donating ligands and M_2 moiety. (B) The dominant electron configuration of the $O_4(W_2)O_4$ complex.

The M-M bonding MOs of the $O_4(W_2)O_4$ complex are also shown in Fig. 4B. The MOs are dominantly localized in the M-M moiety, and the ligand MOs mix only slightly in an anti-bonding manner. These orbital interactions are apparently different from those in the benzene complex shown in Fig. 3B. The O_4 ligand has lone-pair orbitals on the oxygen atoms interacting with M_2 but no electron-accepting orbital in unoccupied space. In contrast, the benzene ligand uses both π and π^* MOs for the interaction with M_2. The π MOs of benzene participates in weakly anti-bonding interactions with the σ_{nd}, π_{nd}, and $\sigma_{(n+1)s}$ MOs, while the π^* MOs form strongly bonding MOs with the δ_{nd} and δ^*_{nd} MOs. As a result, the energy of the δ^*_{nd} MOs becomes lower than that of the $\sigma_{(n+1)s}$ MO in $C_6H_6(M_2)C_6H_6$, which is very bad for the formation of a sextuple bond.

The EBO of the M-M bond in the complexes changes little from that of naked M_2 as seen in Table 1. For example, the EBOs of the $O_4(W_2)O_4$ and $O_4(Mo_2)O_4$ complexes are 5.17 and 5.10, respectively. This result indicates that the W-W and Mo-Mo sextuple bonds are well maintained in these complex. The order of the occupied and unoccupied orbitals does not change with decreasing in the M–O_4 distance; see Fig. 5C. These results show that our ligand design works well. However, the EBO of the $[O_4(Re_2)O_4]^{2+}$ complex was 4.76, and showed a minor change (+0.07). This is because the weight of the S_0 configuration (37%) is considerably smaller than those of the $O_4(W_2)O_4$ (67%) and $O_4(Mo_2)O_4$ (65%) complexes; see Table S2B in ESI, which indicates the presence of strong electron correlations in the $[O_4(Re_2)O_4]^{2+}$ complex because of the presence of the low lying δ^*_{nd} MOs. The $[O_4(Tc_2)O_4]^{2+}$ complex still has a triplet ground state dominated by the $\sigma^1_{(n+1)s}\sigma^2_{nd}\pi^4_{nd}\delta^4_{nd}\sigma^{*0}_{(n+1)s}\sigma^{*0}_{nd}\pi^{*0}_{nd}\delta^{*1}_{nd}$ configuration. Calculated EBO was 4.31, indicating that the sextuple bond cannot be formed with Tc_2^{2+}. These results indicate that the W-W and Mo-Mo sextuple bond is well maintained in these complexes.

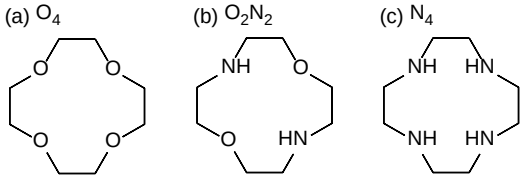

Scheme 1. Structures of (a) 12-crown-4 ether (O_4), (b) 1,7-diaza-12-crown-4 ether (O_2N_2), and (c) 1,4,7,10-tetraza-12-crown-4 ether (N_4)

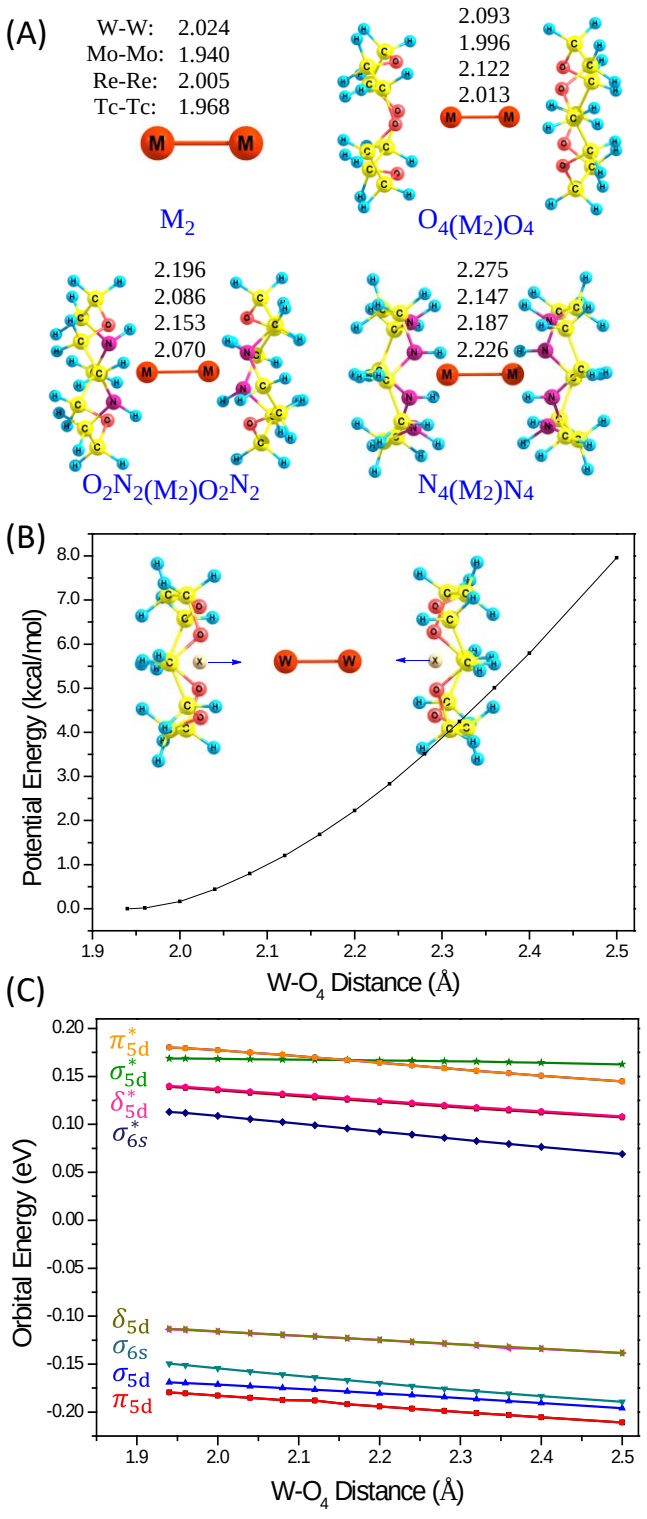

Fig. 5 (A) Structures of the bare M_2 and the dinuclear complexes. The numbers are the metal-metal bond lengths in Å. (B) Potential energy curve of the W–O_4 coordination in S_0 state. (C) Change in orbital energies against W-O_4 distance. The W–O_4 distance is defined as that between W and X (the center of the four O atoms). Calculations were performed with DFT; see section S1 in ESI for computational details.

Though Tc^+ and Mo are isoelectronic pair, their end-on complexes have different spin multiplicities in their ground states. Figure 2 show a schematic diagram of the orbital energy levels and their occupation. Because of the stronger charge transfer interaction between O_4 and Tc^+, the Tc-O distance is shorter than Mo-O distance by 0.48 Å. As a result, the 5s orbital is more destabilized than the 4d orbital, and the σ_{5s} becomes comparable with the δ^*_{5d}. For the Re^+ and W isoelectronic pair, the trend similar to the Tc^+-Mo pair was observed. However, their end-on $O_4(M_2)O_4$ complexes both have singlet ground state because 6s orbital of the 5d transition element becomes more stable due to relativistic effects.[42]

Because the O_4 ligand successfully maintains the sextuple bond, we examined similar neutral tetradentate ligands by substituting two or four O atoms in O_4 with NH groups; they are named O_2N_2 and N_4 ligands, respectively; see Scheme 1 and Fig. 5A for the structures. Similar to the O_4 complexes, all O_2N_2 and N_4 complexes with the W_2, Mo_2, and Re_2^{2+} cores have the S_0 ground state, while the Tc_2^{2+} analogues have a triplet ground state. The EBO of W-W, Mo-Mo, and Re-Re increases in the order $O_4(M_2)O_4$ < $O_2N_2(M_2)O_2N_2$ < $N_4(M_2)N_4$ as shown in Table 1. All the Mo_2, W_2, and Re_2^{2+} complexes with the O_2N_2 and N_4 ligands have an EBO greater than five, indicating that the sextuple bond is formed. For example, the EBO of the $N_4(W_2)N_4$, $N_4(Mo_2)N_4$, and $[N_4(Re_2)N_4]^{2+}$ are 5.51, 5.29, and 5.58, respectively. The increase in EBO mainly arises from the increase in the EBO of the δ_{nd} bonds; see Table 1. As shown in Table S5 in the ESI, the δ^*_{nd}-δ_{nd} energy gap becomes larger when the stronger electron-donating ligand N_4 is used. As a result, the contribution of excited electron configurations to the δ^*_{nd} MOs decreases, and the weight of the sextuply bonded closed-shell configuration, namely S_0 character, increases; for instance, the weight for $N_4(W_2)N_4$, $N_4(Mo_2)N_4$, and $[N_4(Re_2)N_4]^{2+}$ increases by 12.5, 2.0, and 44.8 percent respectively, as shown in Table S2B in ESI.

Possibility of complexes with a side-on-like coordination. In addition to the M_2-end coordination discussed above, we also examined a possibility of an M_2-side coordination; see Fig. 6. In the M_2-side complexes, each metal still coordinates with four atoms of the ligands. The M_2-side $O_4(M_2)O_4$ (M = W_2, Mo_2, and Re_2^{2+}) complexes have quintet ground state, and all M_2-side $O_2N_2(M_2)O_2N_2$ and $N_4(M_2)N_4$ complexes have triplet ground state; see Table S3 in ESI. Only exeption is the M_2-side complex $[O_4(Tc_2)O_4]^{2+}$, which has singlet ground state.

Concerning the energy level of the M_2-side complex relative to the M_2-end complex, the M_2-side complex is less stable than the corresponding M_2-end one by more than 10.0 kcal/mol as shown in Table S3 in ESI. Only exeption is the M_2-side $[O_4(Tc_2)O_4]^{2+}$ complex that is only 5.7 kcal/mol higher than the the corresponding M_2-end complex. Such a small energy gap indicates the two types of structures are thermaldynamicly comparable.

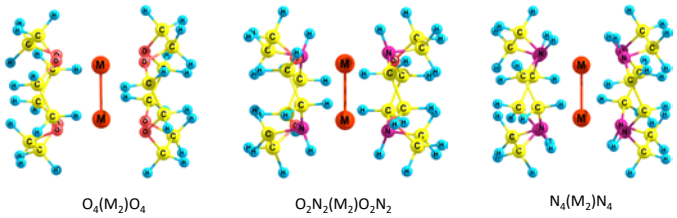

Fig. 6. The structures of the M_2-side $O_4(M_2)O_4$, $O_2N_2(M_2)O_2N_2$, and $N_4(M_2)N_4$ complexes.

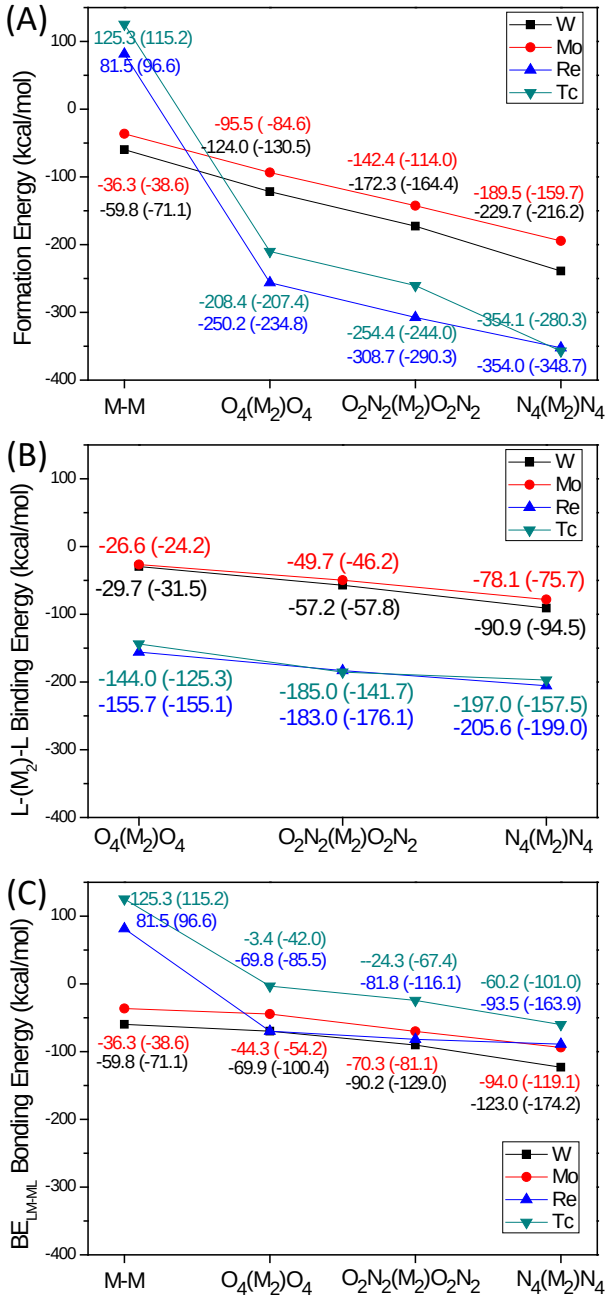

Fig. 7 Formation energy (eq. 2) and binding energy (eqs. 3 and 4) calculated with CASPT2 method. The values in parentheses are calculated by the DFT method. The negative values of the formation energy and the binding energy correspond to the exothermicity. (A) Formation energy. (B) Binding energy, $BE_{\mathrm{L-(M_2)-L}}$. (C) Binding energy, $BE_{\mathrm{LM-ML}}$.

2.3. Thermodynamic stability of sextuply bonded complexes

The formation energy of the complexes. Thermodynamic stability is an important factor to be considered. We evaluated the formation energy of the complexes as follows.

$$\Delta E = E_{opt}[\mathrm{L(M_2)L}] - \{\, 2 \cdot E[\mathrm{M}] + 2 \cdot E_{opt}[\mathrm{L}] \,\} \qquad (2)$$

$E_{opt}[\mathrm{L(M_2)L}]$, $E[\mathrm{M}]$, and $E_{opt}[\mathrm{L}]$ stand for the potential energies of the entire complex, the transition metal atom/cation, and the ligand at their ground-state optimized structures, respectively; see Table S6 and S7.

The formations of the $O_4(W_2)O_4$, $O_4(Mo_2)O_4$, $[O_4(Re_2)O_4]^{2+}$, and $[O_4(Tc_2)O_4]^{2+}$ complexes from separated M and O_4 are exothermic by 124.0, 95.5, 250.2, and 208.4 kcal/mol, respectively, at the CASPT2 level, and 130.5, 84.6, 234.8, and 207.4 kcal/mol, respectively, at the DFT level; see Fig. 7A. The calculated Gibbs formation energies at 298.15 K are 101.2, 52.8, 195.7, and 171.9 kcal/mol, respectively, at the DFT level. It is noteworthy that the formations of the $[O_4(Re_2)O_4]^{2+}$ and $[O_4(Tc_2)O_4]^{2+}$ complexes are significantly exothermic despite the large endothermicity in the Re_2^{2+} and Tc_2^{2+} bond formation. In addition, these dicationic complexes exhibit formation energies larger than those of their neutral W_2 and Mo_2 analogous due to stronger electrostatic interaction between O_4 and the cationic metal center, which will be discussed below. Similar to the O_4 complexes, the calculated formation energies of the O_2N_2 and N_4 complexes are all exothermic as shown in Fig. 7A, indicating their thermodynamic stability.

Metal-ligand and metal-metal bond energies. As described above, the formation energies of the complexes are much larger than those of the bare metal dimers. In addition, the formation energy becomes larger when stronger electron-donating ligands (O_2N_2 and N_4) are used. Fig. 8A shows that the charges in the metal moiety, which is relevant to the donative property of the ligands, correlates well to the formation energy of the complexes. In this subsection, the reasons are analyzed by an energy decomposition. For this purpose, the binding energy between L and M_2 ($BE_{\mathrm{L-(M_2)-L}}$) and the metal-metal bonding energy between two LM moieties ($BE_{\mathrm{LM-ML}}$) were evaluated with the following equations,

$$BE_{\mathrm{L-(M_2)-L}} = \frac{1}{2}\{E_{opt}[\mathrm{L(M_2)L}] - E_{SP}[\mathrm{M_2}] - 2\,E_{SP}[\mathrm{L}]\} \qquad (3)$$

$$BE_{\mathrm{LM-ML}} = E_{opt}[\mathrm{L(M_2)L}] - 2\,E_{SP}[\mathrm{LM}] \qquad (4)$$

where $E_{opt}[\mathrm{L(M_2)L}]$, $E_{SP}[\mathrm{M_2}]$, $E_{SP}[\mathrm{LM}]$, and $E_{SP}[\mathrm{L}]$ are potential energies of the entire complex, the M_2 moiety, the LM moiety, and the ligand, respectively. The subscript, "*SP*", denotes a single-point calculation, in which geometries of M_2, L, and LM were taken to be the same as those of the corresponding moieties of the DFT-optimized structure of $\mathrm{L(M_2)L}$. The ground-state energies were used for all these equations.[60]

As shown in Figs. 7B and 7C, both $BE_{\mathrm{L-(M_2)-L}}$ and $BE_{\mathrm{LM-ML}}$ are negative and contribute to the stabilization of the complex. In Fig. S4 in ESI, the weight of $BE_{\mathrm{L-(M_2)-L}}$ and $BE_{\mathrm{LM-ML}}$ is compared. In neutral W_2 and Mo_2 complexes, the contributions of $BE_{\mathrm{L-(M_2)-L}}$

and $BE_{\mathrm{LM-ML}}$ are comparable, while $BE_{\mathrm{L-(M_2)-L}}$ is significantly larger than $BE_{\mathrm{LM-ML}}$ in cationic Re_2^{2+} and Tc_2^{2+} complexes. The large $BE_{\mathrm{L-(M_2)-L}}$ contribution in the cationic complexes originates from both electrostatic and orbital interactions. As shown in Fig. S5 in ESI, the positive electrostatic potential from the metal core is extending toward outside the M-M moiety. This positive region overlaps very well with the ligand lone-pair electrons. In Fig. S3 in ESI, the electron difference density map by the complex formation is compared between $O_4(W_2)O_4$ and of $[O_4(Re_2)O_4]^{2+}$. The amount of CT from the ligands to the Re_2 core is apparently greater than that to the W_2 core, which indicates that greater orbital interaction leads to larger $BE_{\mathrm{L-(M_2)-L}}$ in the Re complex.

As shown in Fig. 7B, the amount of $BE_{\mathrm{L-(M_2)-L}}$ becomes larger with the increase in the donative property of the ligand (O_4 < O_2N_2 < N_4). This result consistently correlates to the metal-ligand distance as shown in Table S4 in ESI; the M-L distances are in the order of $O_4(M_2)O_4$ > $O_2N_2(M_2)O_2N_2$ > $N_4(M_2)N_4$. In the $O_2N_2(M_2)O_2N_2$ complex, the M-O distance is also longer than the M-N distance, but the deviation between the M-O and M-N distances becomes smaller than those in $O_4(M_2)O_4$ and $N_4(M_2)N_4$ complexes. This trend is rationalized by the orbital interactions. The bonding orbitals between M and L are shown in Fig. S6 in ESI. Apparently, the M-L orbital mixing in the N_4 ligand is larger than that in the O_4 ligand. In Fig. S7 in ESI, lone-pair MOs and their orbital energies are summarized for the O_4, O_2N_2, and N_4 ligands. The averaged energy level of the N_4 lone-pair orbitals (-7.4 eV) is higher than that of the O_4 ligand (-10.2 eV). This feature arises from the fact that the energy of the nitrogen 2p orbital is higher than that of the oxygen 2p and closer to that of the valence d-orbitals of the metal core. As a result, the $BE_{\mathrm{L-(M_2)-L}}$ for the N_4 ligand becomes larger than that for the O_4 ligand. The orbital interaction affects the calculated M-L distance. As shown in Table S4 in ESI, the M-N_4 distance is shorter than that of the M-O_4 one. For example, the calculated W-L distance for the N_4, O_2N_2, and O_4 ligands is 2.4 Å, 2.5 Å, and 2.8 Å, respectively.

As shown in Fig. 7C, the amount of $BE_{\mathrm{LM-ML}}$ increases with the increase in the donative property of the ligand (O_4 < O_2N_2 < N_4). Fig 8B also indicates that $BE_{\mathrm{LM-ML}}$ increases with the electron population around the metal moiety. This trend correlates to the EBO for the δ-bond. For instance, $\mathrm{EBO}\delta_{nd}$ for the $N_4W_2N_4$ complex (1.80) is larger than that for $O_4(W_2)O_4$ complex (1.52). This is because the occupation number of the δ_{nd} orbitals increases and that of the δ^*_{nd} orbitals decreases. The occupation number of the two δ_{nd} orbitals are 3.79 for $N_4(W_2)N_4$ and 3.52 for $O_4(W_2)O_4$, while that for the two δ^*_{nd} orbitals are 0.20 for $N_4W_2N_4$ and 0.47 for $O_4W_2O_4$; see Fig S9 in ESI. These changes in the occupation number indicate that the weight of the δ-δ^* excited configurations decreases significantly because the δ-δ^* orbital energy gap is increased by the N_4 ligand. The averaged δ-δ^* gap is 8.1 eV and 6.9 eV for $N_4W_2N_4$ and $O_4W_2O_4$, respectively; see Table S5 in ESI. This increase in the gap mainly arises from the destabilization of the δ^* orbital by 0.8 eV. The CASSCF natural orbitals for $O_4(W_2)O_4$ and $N_4(W_2)N_4$ (Fig. S9 in ESI) clearly show that the metal-ligand anti-bonding interaction in $N_4W_2N_4$ is larger than that in $O_4(W_2)O_4$. The increasing order in the δ-δ^* orbital energy gap O_4 < O_2N_2 < N_4 arises from the stronger σ-donating natures of O_2N_2 and N_4 than that of O_4, indicating the use of donating ligand is crucial. We note that, in the previous study, the role of the electrostatic effect was also pointed out for the M-M bond in R_3M–$M'R_3$ (M, M' = Cr, Mo, W; R = Cl, NMe2), $[Re_2Cl^8]^{2-}$, and Os_2Cl_8 complexes by using the EDA/EDA-NOCV analysis.[23, 61, 62] Because the donative ligands increase the charges on the metal moiety, the electrostatic interpretation should be a rational interpretation.

In addition, the BE_{LM-ML} values of the W_2 and Re_2^{2+} complexes are larger than those of the Mo_2 and Tc_2^{2+} complexes in most cases; see Fig. 7C. This is attributed to the stronger $\sigma_{(n+1)s}$ bonding interaction in the W_2 and Re_2^{2+} complexes; see $\mathrm{EBO}\sigma_{(n+1)s}$ in Table 1. This is true because their 6*s* orbitals are more stable than the 5*s* orbitals of Mo and Tc due to relativistic effects.[42]

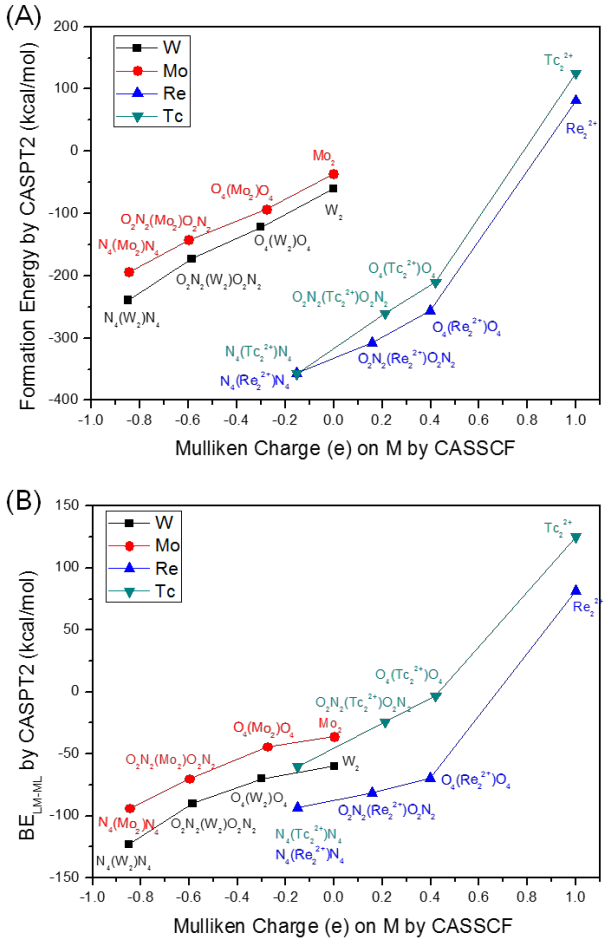

Fig. 8 The correlation of (A) formation energy and (B) $BE_{\mathrm{LM-ML}}$ with calculated atomic charge of transition metal.

It would be worth comparing the present complexes with an existing quintuply bonded complex. The HOMO and LUMO levels of $Mo_2(N^N)_2$ ({N^N = μ-κ^2-CH[N(2,6-*i*Pr$_2$C$_6$H$_3$)]$_2$}) was calculated to be -6.13 eV and 0.05 eV, respectively, in our previous work.[63] The HOMO-LUMO energy gap of the end-on complexes are smaller than that of $Mo_2(N^N)_2$ except for the Re_2 complexes; see Table S9. For example, the gaps of $O_4(Mo_2)O_4$, $N_2O_2(Mo_2)N_2O_2$, $N_4(Mo_2)N_4$ are 4.26 eV, 3.55 eV, and 3.54 eV, respectively. These results indicate the sextuply bonded is likely to be more reactive compared with the

quintuply bonded complex $Mo_2(N^N)_2$. In addition, the HOMO level of those neutral complexes is higher than that of $Mo_2(N^N)_2$. For example, the HOMO energy of $O_4(Mo_2)O_4$, $N_2O_2(Mo_2)N_2O_2$, $N_4(Mo_2)N_4$ are -3.19 eV, -2.50 eV, and -2.51 eV, respectively, implying that these neutral complexes may perform well as an electron donor.

The thermodynamic stability of mono-nuclear complex. There is a possibility that the formation of two mono-nuclear complexes competes with that of dinucear complex. The Gibbs formation energies are 0.6, 5.3, and -95.6 kcal/mol for $O_4(W)O_4$, $O_4(Mo)O_4$, $O_4(Re^+)O_4$, respectively, while those for the corresponding dinuclear complexes are -101.2, -52.8 and -195.7 kcal/mol at DFT level; see Table S8 in ESI. The significant difference in the Gibbs formation energy between the mono-nuclear and dinuclear complexes mainly arises from the metal-metal bonding interaction. These results also indicate the possibility of the synthesis of the dinuclear complexes.

3. Conclusions

We theoretically proposed a molecular-designing strategy for realizing stable metal-metal sextuply-bonded complexes for the first time. The present coordination strategy is based on the following ideas: Stabilizing the M_2 core by the ligand coordination, conserving the six bonding orbitals in the occupied space, and suppressing the δ-δ^* electron correlations.

The state-of-the-art CASPT2 and DFT calculations showed that the tetradentate electron-donating ligands, such as O_4, O_2N_2, and N_4, can enhance thermodynamic stability, keeping the Mo-Mo and W-W sextuple bonds like in the bare metal dimers. Even $[N_4(Re_2)N_4]^{2+}$ and $[O_2N_2(Re_2)O_2N_2]^{2+}$ could have a Re-Re sextuple bond with the S_0 ground state. All these sextuply bonded complexes have a large formation energy, indicating their thermodynamic stability and possibility of being synthesized. The DFT results were consistent to those from the CASPT2/CASSCF calculations, which indicates that DFT method is applicable to the investigation of the metal-metal multiple bond that can be described by a single-reference electronic structure method. We note that verification with multi-reference methods should improve the reliability of the conclusion. We also note that only multi-reference methods are applicable to the metal-metal bond with a quasi-degenerate electronic structure (see ref. 47 for the U_2 case).

The reason of the stability has been analyzed in detail. The stabilization energy arises from both metal-metal binding and metal-ligand binding. As the donative property of the ligand increases, electron population in the δ^*_{nd} orbitals is suppressed because the strong metal-ligand interaction by donating ligand destabilizes the δ^*_{nd} orbital energy. The N_4 ligand can make M-L interaction stronger than does the O_4 ligand because the energy levels of the lone-pair electrons of the N_4 ligand are higher than those of the O_4 ligand and closer to those of the valence d-orbitals.

As mentioned before, quintuply bonded $Mo_2(N^N)_2$ was synthetized in THF solution. We hope that a series of dinuclear complexes proposed in this study are synthesized not in far future.

Acknowledgements

This study was supported by JSPS KAKENHI (Grant Number JP15H05805, JP15H05797, JP15H03770, JP15H00940) and the FLAGSHIP2020, MEXT within priority study 5. A part of the computations was performed at RCCS (Okazaki, Japan) and ACCMS (Kyoto University).

Notes and references

1. G. Frenking and R. Tonner, *Nature*, 2007, **446**, 276-277.
2. S. Shaik, D. Danovich, W. Wu, P. Su, H. S. Rzepa and P. C. Hiberty, *Nat. Chem.*, 2012, **4**, 195-200.
3. S. Shaik, H. S. Rzepa and R. Hoffmann, *Angew. Chem. Int. Ed.*, 2013, **52**, 3020-3033.
4. D. Danovich, P. C. Hiberty, W. Wu, H. S. Rzepa and S. Shaik, *Chem. -Eur. J.*, 2014, **20**, 6220-6232.
5. F. A. Cotton, *Inorg. Chem.*, 1965, **4**, 334-336.
6. T. Nguyen, A. D. Sutton, M. Brynda, J. C. Fettinger, G. J. Long and P. P. Power, *Science*, 2005, **310**, 844-847.
7. F. R. Wagner, A. Noor and R. Kempe, *Nat. Chem.*, 2009, **1**, 529-536.
8. N. V. S. Harisomayajula, A. K. Nair and Y.-C. Tsai, *Chem. Commun.*, 2014, **50**, 3391-3412.
9. A. Noor and R. Kempe, *Chem. Rec.*, 2010, **10**, 413-416.
10. Y.-C. Tsai, H.-Z. Chen, C.-C. Chang, J.-S. K. Yu, G.-H. Lee, Y. Wang and T.-S. Kuo, *J. Am. Chem. Soc.*, 2009, **131**, 12534-12535.
11. Y.-C. Tsai, Y.-M. Lin, J.-S. K. Yu and J.-K. Hwang, *J. Am. Chem. Soc.*, 2006, **128**, 13980-13981.
12. K. A. Kreisel, G. P. A. Yap, O. Dmitrenko, C. R. Landis and K. H. Theopold, *J. Am. Chem. Soc.*, 2007, **129**, 14162-14163.
13. G. Merino, K. J. Donald, J. S. D'Acchioli and R. Hoffmann, *J. Am. Chem. Soc.*, 2007, **129**, 15295-15302.
14. S. Horvath, S. I. Gorelsky, S. Gambarotta and I. Korobkov, *Angew. Chem.*, 2008, **120**, 10085-10088.
15. C.-W. Hsu, J.-S. K. Yu, C.-H. Yen, G.-H. Lee, Y. Wang and Y.-C. Tsai, *Angew. Chem. Int. Ed.*, 2008, **47**, 9933-9936.
16. A. Noor, F. R. Wagner and R. Kempe, *Angew. Chem. Int. Ed.*, 2008, **47**, 7246-7249.
17. S.-C. Liu, W.-L. Ke, J.-S. K. Yu, T.-S. Kuo and Y.-C. Tsai, *Angew. Chem. Int. Ed.*, 2012, **51**, 6394-6397.
18. M. Brynda, L. Gagliardi, P.-O. Widmark, P. P. Power and B. O. Roos, *Angew. Chem.*, 2006, **118**, 3888-3891.
19. G. Li Manni, A. L. Dzubak, A. Mulla, D. W. Brogden, J. F. Berry and L. Gagliardi, *Chem. -Eur. J.*, 2012, **18**, 1737-1749.
20. A. Noor, G. Glatz, R. Müller, M. Kaupp, S. Demeshko and R. Kempe, *Z. Anorg. Allg. Chem.*, 2009, **635**, 1149-1152.
21. M. Carrasco, M. Faust, R. Peloso, A. Rodriguez, J. Lopez-Serrano, E. Alvarez, C. Maya, P. P. Power and E. Carmona, *Chem. Commun.*, 2012, **48**, 3954-3956.
22. G. La Macchia, G. Li Manni, T. K. Todorova, M. Brynda, F. Aquilante, B. O. Roos and L. Gagliardi, *Inorg. Chem.*, 2010, **49**, 5216-5222.
23. N. Takagi, A. Krapp and G. Frenking, *Inorg. Chem.*, 2011, **50**, 819-826.
24. A. Noor, G. Glatz, R. Müller, M. Kaupp, S. Demeshko and R. Kempe, *Nat. Chem.*, 2009, **1**, 322-325.
25. C. Ni, B. D. Ellis, G. J. Long and P. P. Power, *Chem. Commun.*, 2009, **0**, 2332-2334.
26. P. F. Wu, S. C. Liu, Y. J. Shieh, T. S. Kuo, G. H. Lee, Y. Wang and Y. C. Tsai, *Chem. Commun.*, 2013, **49**, 4391-4393.

27. C. Schwarzmaier, A. Noor, G. Glatz, M. Zabel, A. Y. Timoshkin, B. M. Cossairt, C. C. Cummins, R. Kempe and M. Scheer, *Angew. Chem. Int. Ed.*, 2011, **50**, 7283-7286.
28. E. S. Tamne, A. Noor, S. Qayyum, T. Bauer and R. Kempe, *Inorg. Chem.*, 2012, **52**, 329-336.
29. A. Noor, E. Sobgwi Tamne, S. Qayyum, T. Bauer and R. Kempe, *Chem. -Eur. J.*, 2011, **17**, 6900-6903.
30. J. Shen, G. P. A. Yap, J.-P. Werner and K. H. Theopold, *Chem. Commun.*, 2011, **47**, 12191-12193.
31. H.-Z. Chen, S.-C. Liu, C.-H. Yen, J.-S. K. Yu, Y.-J. Shieh, T.-S. Kuo and Y.-C. Tsai, *Angew. Chem. Int. Ed.*, 2012, **51**, 10342-10346.
32. Y. Chen and S. Sakaki, *Dalton Trans.*, 2014, **43**, 11478-11492.
33. M. Carrasco, N. Curado, C. Maya, R. Peloso, A. Rodríguez, E. Ruiz, S. Alvarez and E. Carmona, *Angew. Chem. Int. Ed.*, 2013, **52**, 3227-3231.
34. H.-G. Chen, H.-W. Hsueh, T.-S. Kuo and Y.-C. Tsai, *Angew. Chem. Int. Ed.*, 2013, **52**, 10256-10260.
35. M. M. Goodgame and W. A. Goddard, *J. Phys. Chem.*, 1981, **85**, 215-217.
36. Y. Kitagawa, Y. Nakanishi, T. Saito, T. Kawakami, M. Okumura and K. Yamaguchi, *Int. J. Quant. Chem.*, 2009, **109**, 3315-3324.
37. M. Brynda, L. Gagliardi and B. O. Roos, *Chem. Phys. Lett.*, 2009, **471**, 1-10.
38. P. M. Atha, I. H. Hillier and M. F. Guest, *Chem. Phys. Lett.*, 1980, **75**, 84-86.
39. A. C. Borin, J. P. Gobbo and B. O. Roos, *Chem. Phys.*, 2008, **343**, 210-216.
40. B. E. Bursten, F. A. Cotton and M. B. Hall, *J. Am. Chem. Soc.*, 1980, **102**, 6348-6349.
41. D. Kraus, M. Lorenz and V. E. Bondybey, *PhysChemComm*, 2001, **4**, 44-48.
42. Y.-L. Wang, H.-S. Hu, W.-L. Li, F. Wei and J. Li, *J. Am. Chem. Soc.*, 2016, **138**, 1126-1129.
43. C. Angeli, A. Cavallini and R. Cimiraglia, *J. Chem. Phys.*, 2007, **127**, 074306.
44. Z. J. Wu and X. F. Ma, *Chem. Phys. Lett.*, 2003, **371**, 35-39.
45. A. C. Borin, J. P. Gobbo and B. O. Roos, *Chem. Phys. Lett.*, 2010, **490**, 24-28.
46. E. A. Boudreaux and E. Baxter, *Int. J. Quant. Chem.*, 2004, **100**, 1170-1178.
47. L. Gagliardi and B. O. Roos, *Nature*, 2005, **433**, 848-851.
48. G. La Macchia, M. Brynda and L. Gagliardi, *Angew. Chem. Int. Ed.*, 2006, **45**, 6210-6213.
49. B. O. Roos, P.-Å. Malmqvist and L. Gagliardi, *J. Am. Chem. Soc.*, 2006, **128**, 17000-17006.
50. L. Gagliardi, P. Pyykko and B. O. Roos, *Phys. Chem. Chem. Phys.*, 2005, **7**, 2415-2417.
51. D. A. Penchoff and B. E. Bursten, *Inorg. Chim. Acta*, 2015, **424**, 267-273.
52. C.-Z. Wang, J. K. Gibson, J.-H. Lan, Q.-Y. Wu, Y.-L. Zhao, J. Li, Z.-F. Chai and W.-Q. Shi, *Dalton Trans.*, 2015, **44**, 17045-17053.
53. K. Saito, Y. Nakao, H. Sato and S. Sakaki, *J. Phys. Chem. A*, 2006, **110**, 9710-9717.
54. B. O. Roos, A. C. Borin and L. Gagliardi, *Angew. Chem. Int. Ed.*, 2007, **46**, 1469-1472.
55. B. O. Roos, *Collect. Czech. Chem. Commun.*, 2003, **68**, 265-274.
56. B. Xu, Q.-S. Li, Y. Xie, R. B. King and H. F. Schaefer, *J. Chem. Theory Comput.*, 2010, **6**, 735-746.
57. Z. Sun, H. F. Schaefer, Y. Xie, Y. Liu and R. Zhong, *Mol. Phys.*, 2013, **111**, 2523-2535.
58. R. Reichenbach-Klinke and B. Konig, *J. Chem. Soc. Dalton Trans.*, 2002, 121-130.
59. L. Yu, F.-z. Li, J.-y. Wu, J.-q. Xie and S. Li, *J. Inorg. Biochem.*, 2016, **154**, 89-102.
60. *The ground state of the LM fragment was in septet spin multiplicity.*
61. A. Krapp, M. Lein and G. Frenking, *Theor. Chm. Acc.*, 2008, **120**, 313-320.
62. M. v. Hopffgarten and G. Frenking, *Wiley Interdisciplinary Reviews: Computational Molecular Science*, 2012, **2**, 43-62.
63. Y. Chen and S. Sakaki, *Inorg. Chem.*, 2017, **56**, 4011-4020.